Autoinduction through the coupling of nucleation-dependent self-assembly of a supramolecular gelator and a reaction network†

Jamie S. Foster[a] and Gareth O. Lloyd [iD] *[b]

Autocatalytic and/or self-replicating systems are important aspects of understanding the link between living systems (origins of life) and chemical networks. As a result, many scientists around the world are attempting to better understand these phenomena by producing chemical networks and linking them to self-assembly and pathway complexity (systems chemistry). We present here a superficially autocatalytic, self-replicating system that utilises dynamic imine chemistry coupled with self-assembling supramolecular hydrogelation kinetics driven by a nucleation autocatalytic cycle (autoinduction). The dynamic nature of the imine bond within water allows "error-checking" correction and driving of the imine equilibrium to the starting materials, but when coupled to the self-assembly process it gives rise to one reaction product from a possible thirteen intermediates and/or products (of a mixed four-step reaction). This product represents a thermodynamic minimum within the system's and reaction network's energy landscape. The self-assembly in solution of the replicator results in the formation of supramolecular polymers, which would normally markedly reduce the catalytic efficiency of the system if a template mechanism of autocatalysis is in play. By overcoming the limiting effects of the self-assembly process, it is possible to demonstrate exponential growth in replicator concentration once nucleation has occurred. It is only once the completed imine can undergo non-reversible tautomerisation that the product is prevented from reacting with water. We thus suggest that this sigmoidal kinetic characterisation is not inherent to autocatalysis kinetics (lowering reaction barriers and/or templating), but rather a result of the nucleation-based assembly allowing for intermediates to be prevented from reacting with water in a water-deficient environment (an autoinduction autocatalytic mechanism). Not only does this study provide a basis with which to explore aspects of self-replication connected with self-assembly, but it also explores how nucleation and

[a]*Institute of Chemical Sciences, School of Engineering and Physical Sciences, Heriot-Watt University, Edinburgh, Scotland, EH14 4AS, UK*

[b]*Department of Chemistry, School of Natural Sciences, Joseph Banks Laboratories, Lincoln, LN6 7DL, UK. E-mail: glloyd@lincoln.ac.uk*

† Electronic supplementary information (ESI) available. See DOI: https://doi.org/10.1039/d5fd00016e
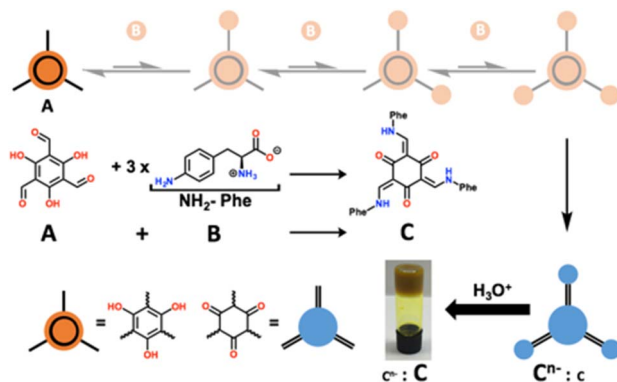
self-assembly growth can play a crucial role in self-replication. By controlling the kinetics of the autocatalytic chemical reaction at one end of the hierarchical assembly process, we can influence the physical properties of the supramolecular gel at the other end. This may have wide-ranging applications with *in-situ*-formed small molecular gelators where specific mechanical properties (rheology) are desired.

Introduction

Self-replication, or autocatalysis, relating to autoinduction is a keystone of chemical biology and is an important concept in the understanding of chemical complexity.[1–3] Supramolecular chemistry has long been recognised as a key part of the process involved in an autocatalytic chemical reaction. The well-recognised design principle of template-directed ligation of reactant components of the replicator/product describes this supramolecular recognition function.[1–3] However, subsequent dissociation of this duplex formed after linkage of the building blocks between "two" products is necessary if exponential growth of the replicator is to be seen.[4] This exponential growth results from the liberation of two replicators from the duplex that can each mediate another round of replication. When coupled to a dynamic bond formation, replication can inhibit the thermodynamic equilibration of the system.[5] With this in mind, designing biomimetic gelatinous materials such as hydrogels has necessarily included aspects of systems chemistry.[6–9] This has been due to nature's exquisite ability to control assembly and disassembly, often resulting in non-equilibrium states.[10–12] This control by nature often arises from catalysed chemical processes, most of which show autocatalytic behaviour. The most successful examples of biomimicry in gelation by small molecule gels to date have included dissipating materials, chemical Darwinian-selection, and catalysed formation.[13] There has also been a keen increase in interest on the self-assembly of peptides (amyloid fibrils in particular) that occurs *via* autocatalytic assembly, and there has been a recognised association of the nucleation/growth kinetics to these processes.[14] This, connected with classical nucleation theory, shows that crystal growth or nucleation determine that self-assembly processes are naturally autocatalytic in terms of their kinetics.[15] However, there are relatively few autocatalytic gelation[16] or supramolecular polymerisation processes described so far with simple building blocks.[17] Therefore, we aimed to produce and study an autocatalytic reaction involved in a gel-forming process that may be valuable in studies of biomimetic gelation and the resultant materials by coupling a reaction network with an autocatalytic nucleation-based self-assembly (Scheme 1).[18,19] We have used a combination of the core **A** (1,3,5-triformylglucinol) and periphery **B** (4-amino-L-phenylalanine) that react together through the imine dynamic covalent chemistry resulting in the potential reaction network. The reaction network, however, only appears to form one observable product, and no other potential product nor intermediate is observed, unusually. By developing an understanding of these reaction kinetics for the formation of the individual supramolecular building blocks we hoped to be able to control the physical properties, such as mechanical strength, of any resulting gel.[20] Control would arise from trapping a specific concentration of the gelator through a mass transfer limitation mechanism (Le Chatelier's principle), stopping the reaction reaching completion.[21] A necessitated

Scheme 1 Simplified linear reaction scheme for the reaction, from combination of the starting materials, **A** (1,3,5-triformylglucinol) and **B** (4-amino-L-phenylalanine). Mixing of **A** and **B** occurs in water at pH 8 and results in formation of the deprotonated non-gelating but supramolecular-fibre-assembling species C^{n-}. Acidification of C^{n-} results in protonation, giving rise to the formation of the low molecular weight gelator (LMWG) **C**.

discussion based on what gives rise to these perceived autocatalytic kinetics when we connect our reaction networks and self-assembly will also be presented, and again there appears to be a connectivity between nucleation/growth self-assembly, Le Chatelier's principle, and equilibria of the reactions.

Results and discussion

The design of our self-replicating system is based on the initial formation of imine bonds. There are two processes on which the system is reliant. The classic imine dynamic covalent chemistry involving the aldehyde and amine groups,[22] followed by an enol–keto tautomerisation (Scheme 1 and Fig. S1†). Mixing **A** and **B** in water at pH 9 gives only one isolatable product, C^{n-}. We propose the dynamic nature of the imine bond results in a system where the mono-, di- and tri-imine species are not observed due to their lack of thermodynamic stability. However, reaction to form the tri-reacted imine may induce an enol-imine to keto-enamine tautomerization.[23] This traps the tri-reacted species in the keto tautomeric form, C^{n-}.[24] This species represents a thermodynamic minimum for the reaction between **A** and **B** (Scheme 1). The amino acid **B** features two amine groups, both having the potential to react with the aldehyde groups of **A**. However, spectroscopic evidence (see the ESI, Fig. S9 and S10†) shows only one product resulting from the reaction at the aromatic amine of **B** to give C^{n-}. And we believe the alternative products where the alkyl amine has reacted with an aldehyde would result in a highly soluble compound that cannot self-assemble at this pH in water, driving its equilibrium formation back to the starting material under these conditions.

The formation of C^{n-} could be monitored by HPLC and ^{1}H NMR (Sections 9, 14, 15 and 18 of the ESI†). This was done in water with standard experimental conditions of pH 9 at 20 °C. The HPLC analysis measured absorption at 290 nm at retention times corresponding to **A** and C^{n-}. ^{1}H NMR analysis focused on the conversion of the aldehyde peak of **A** at 9.6 ppm to the enamine peak of C^{n-} at 7.5 ppm.

Two solutions containing **A** (28 mM) and an excess of **B** take 72 hours after mixing to completely react to form $\mathbf{C^{n-}}$. A plot of $[\mathbf{C^{n-}}]$ against time gives rise to a sigmoidal profile that suggests an autocatalytic process (Fig. S13 and S16†). A subsequent plot of the calculated autocatalysis with additional templating (product or seeds) can show the true nature of the kinetics (eqn (1)), either autocatalytic or reduce catalyst efficiency as replicator molecules may form dimers or higher ordered structures. This results in the system showing a non-exponential increase in product concentration, $0.5 \leq p < 1$; such a system's growth is said to be parabolic. To determine the order of the reaction, in terms of product concentration, the reaction was seeded with varying concentrations of previously isolated $\mathbf{C^{n-}}$ and the initial rate of $\mathbf{C^{n-}}$ formation was calculated (Fig. S14, S17 and S20†). von Kiedrowski showed that by plotting $\log \mathrm{d}[\mathbf{C^{n-}}]/\mathrm{d}t$ against $\log[\mathbf{C^{n-}}]$, where $[\mathbf{C^{n-}}]$ refers to the concentration of the seed added, p can be determined from the gradient of the line. We therefore determined the relationship, where the reaction rate for $\mathbf{C^{n-}}$ formation $(\mathrm{d}[C]/\mathrm{d}t)$ against time results in a bell-shaped profile, again indicative of autocatalysis.[6,25]

$$\frac{\mathrm{d}[\mathbf{C^{n-}}]}{\mathrm{d}t} = k[\mathbf{C^{n-}}]^p + x \tag{1}$$

Eqn (1), above, is the general rate equation for an autocatalytic process.[25] $k[\mathbf{C^{n-}}]^p$ is the autocatalytic term, x is the non-autocatalysed reaction and p is the order of reaction with respect to the product. When $p = 1$, an autocatalytic system will exhibit an exponential increase in product concentration. The reliance of rate $= 2.3[\mathbf{C^{n-}}]^1$ (Fig. 1). We can see $p = 1$, thus showing that seeding resulted in an autocatalytic system with an exponential increase in product/replicator occurring.

The face-to-face, π–π stacking of $\mathbf{C^{n-}}$ molecules, evident in the powder X-ray diffraction patterns of dried samples (Fig. S34 and S35†), is proposed as the supramolecular interaction in the product template-based self-assembly and must be evident during a mechanism for the autocatalytic kinetics.[26] The efficiency of the catalytic process relies on the number of accessible faces of $\mathbf{C^{n-}}$ molecules in solution. As the reaction progresses, it is possible to measure an increase in reaction solution viscosity, an indication of the supramolecular polymerisation of $\mathbf{C^{n-}}$. Utilising isolated **C** and dissolving it in pH 9 water, an increasing concentration of $\mathbf{C^{n-}}$ in solution also results in an increase in viscosity. The viscosity of the solution shows a dramatic reduction at temperatures >30 °C. This results from dissociation of the π–π stacking interactions between monomers of $\mathbf{C^{n-}}$ that have formed supramolecular polymers.

There are two methods by which propagation of the supramolecular polymers can occur during the reaction: the conglomeration of individual $\mathbf{C^{n-}}$ molecules in solution that form through the non-catalysed process, and/or inclusion of an intermediate of the reaction network into the polymer chains potentially catalysing the formation of $\mathbf{C^{n-}}$.

The $\mathbf{C^{n-}}$ molecules that form through the reaction process and are part of the supramolecular polymers may fail to dissociate from the polymer, resulting in an increase in polymer length. The presence of supramolecular polymers results in the effectiveness of the autocatalytic process observed experimentally being much lower than the theoretical maximum, as each static linear polymer chain only has
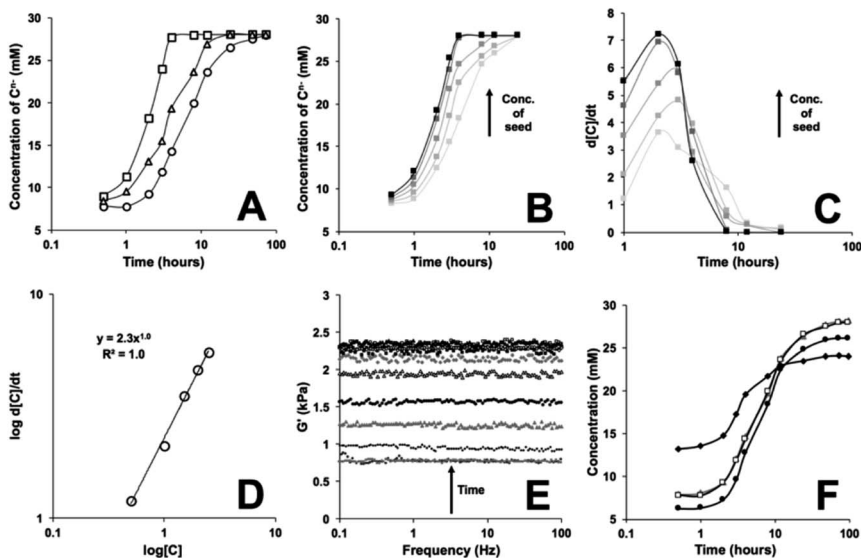
Fig. 1 Data for the autocatalytic reaction to produce C^{n-} and the mechanical properties arising from the hydrogel. Graph A shows $[C^{n-}]$ over time. Standard conditions (○), stirring at 1000 rpm (△), addition of previously isolated C seed at a concentration of 2.5 mM (□). Graph B shows $[C^{n-}]$ increase over time with increasing [seed]. Graph C shows the rate of formation of C^{n-} over time with increasing concentration of seeding C^{n-}. Graph D shows the initial rate of formation of C^{n-} plotted against concentration of seeding C^{n-}. Graph E shows the results of frequency–sweep experiments for gels set at different times after the initial mixing of **A** and **B** and the subsequent acidification to form **C** (coloured version, Fig. S12,† with clearer legends available). 0.5 h ○, 1 h ■, 2 h ◆, 3 h ▲, 4 h ●, 8 h △, 12 h ◆, 24 h ■, 48 h ◇, 72 h □, 96 h ◆. Graph F shows $[C^{n-}]$ over time determined by UV–vis spectroscopy ●, HPLC □, ^{1}H NMR spectroscopy ▲, and rheology using the cellular solid model ◆.

two catalytically active end molecules/sites. It is well recognised now that this addition catalytically (similar to the template process of self-replication) would not lead to the kinetics observed. In our reactions, the replicator:product "duplexes" must be dynamic and related to the supramolecular polymerisation, as described by Otto and co-workers in their description of the fibre elongation/breakage mechanism, and many others who have observed autocatalytic kinetics during the self-assembly of supramolecular polymers/fibrils.[27] In an attempt to mitigate the effects of the supramolecular polymer formation on the perceived catalytic activity, the solution was subjected to physical agitation (stirring at 1000 rpm with a magnetic stirrer; see ESI Sections 12 and 13† for details).[26] Stirring of the solution was started immediately on mixing **A** and **B** and continued until the maximum concentration of C^{n-} was reached. With stirring, the reaction completed within 24 hours, much quicker than the same reaction without stirring. This confirms the autocatalytic kinetics is related to some form of assembly process, as stirring breaks/sheers the polymer chains into smaller units, increasing the number of accessible sites for chemical assembly or reactivity (we cannot determine which). With these observations, data, chemical reactivity, self-assembly, and unknowns in hand, we are naturally led to a discussion (hyperbole)
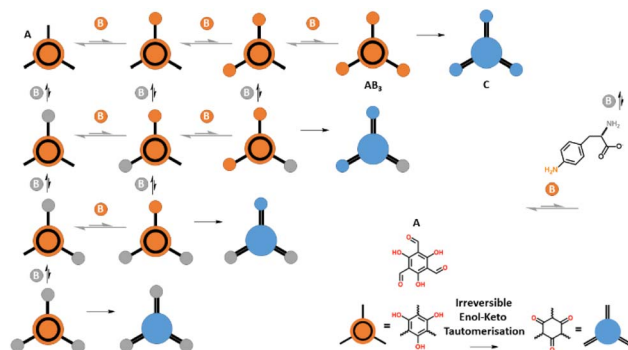
Fig. 2 Reaction network showing the thirteen possible products from the mixing of **A** (1,3,5-triformylglucinol) and **B** (4-amino-L-phenylalanine) in water at a pH of approximately 8. **A** can react with **B** through the aniline functional group (horizontal equilibrium arrows (orange)) or the alkyl amine functional group (vertical equilibrium arrows (grey)). Both equilibria are biased towards starting materials due to water. The irreversible enol–keto tautomerisation only occurs once all three aldehyde functional groups have reacted, shown as a horizontal reaction unidirectional arrow. Only the product **C** is analytically observed. It results from the tautomerisation of AB_3 (the thrice-reacted aniline product).

of how do we describe this connectivity between the reaction network and self-assembly arising in an autoinduction observation.[1]

We can divide this discussion into two parts: (1) are any of the reaction steps (Fig. 2) catalytically enhanced during the process resulting in a self-replication mechanism; (2) is the self-assembly autocatalytic in nature (Fig. 3) and is there
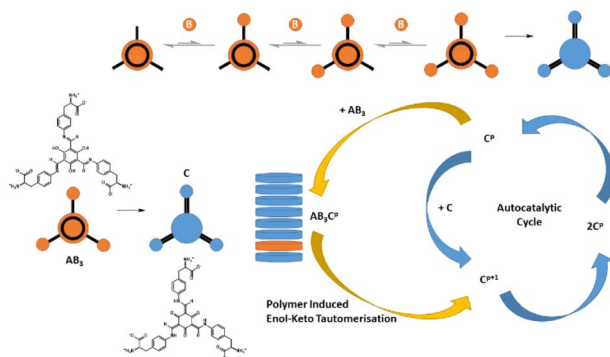

Fig. 3 Autoinduction. The product **C** is formed from AB_3 in a linear reaction pathway of little complexity, with the final reaction of the enol–keto tautomerisation being irreversible. For the kinetics to show sigmoidal rates, we suggest that the tautomerisation is coupled to an autocatalytic cycle (autoinduction). The autocatalytic cycle is the supramolecular polymers. We hypothesise that this is coupled to the coassembly of AB_3 into supramolecular polymers of the final product **C**, thus producing an environment that is favourable to the conversion of AB_3 to **C** (a polymer-induced enol–keto tautomerisation due to the Le Chatelier's principle as the chemical environment would be essentially devoid of water, biasing the equilibrium that is driving AB_3 back to the starting materials). It is easy to envision the coassembly of AB_3 and **C** due to their very similar chemical structures.

a connectivity between the reaction network and this autocatalytic assembly cycle?

The first reflexion of the reaction to take note of is that there is no analytical observation of any of the intermediates of the reaction network. This is a classic analytical limitation of many chemical reactions (most reactions have timescales/kinetics far quicker than most analytical tools) but is unusual given the network possibilities (13 intermediates and/or products, plus an additional five unlikely products associated with the tautomerisation of the five intermediates with free aldehyde groups). An additional fact is the reaction takes three days to complete. We and many others often observe intermediates of complex networks, so why do we not with this one?[21] We postulate that the majority of the intermediates are unstable and transient within the water environment of the reaction, water (which is at its maximum chemical activity as both the solvent and reactant) driving the breaking of any imine formation back to starting materials (in terms of equilibrium chemistry, the water concentration (activity) is unbalancing the equilibrium away from product formation). If there was a template/autocatalytic process occurring with an intermediate and the final product (which clearly has the capacity to cause autoinduction by observation of the seeding process), then we can argue that something observable would be analytically determined so there is a high likelihood of there being no need or possibility for a templated autocatalytic chemical process as part of the imine equilibrium chemistry, except for the potential of the enol–keto tautomerisation. The chemistry presented in this discussion is well recognised as a non-reversible (normally thermally induced)[21a,28] reaction that is not the reaction between two or more reactants but simply a conversion between two compounds that normally has a significant kinetic barrier. Enol–keto tautomerisations are normally in equilibrium and for the chemistry presented it has been observed to be different in water than in other chemical environments (not thermally induced and can be made reversible through an acid:base switch in certain circumstances).[21a,28,29] Indeed, the chemistry has been used to make materials that are chemically inert to water. For the aniline derivatives we have worked with and published, we do not observe the enol form. Therefore the presence of water and salts (H^+, OH^- and Na^+) are likely enhancing (catalysing) the enol–keto tautomerisation, as has been seen in many sugar chemistries (probably the most important autocatalytic process in regard to origin of life chemistries).

In most sugar chemistries that show autocatalytic behaviour (like the Breslow cycle), the products can be reincorporated into the reaction cycle/network. This is not possible for this chemistry and a template mechanism is the only option for generating an autocatalytic cycle. This reaction may be catalysed by the intermediate imine interacting with its product (the enol–keto process), and with water and the other constituents of the solution resulting in enhanced enol–keto tautomerisation. If we take our linear reaction steps from **A** and **B** to the two intermediates then to the thrice-reacted enol, we could potentially observe the simplest template-led autocatalytic chemistry for the tautomerisation. However, the product forms supramolecular polymers, and polymerisation is a known mechanism for poisoning a template autocatalysis reaction. Therefore, we think that we can preclude an in-solution template autocatalytic process. And therefore our focus should be put onto how the self-assembly may induce autocatalysis and the observed autoinduction (discussion point (2)) (Fig. 3).

Can the self-assembly of supramolecular polymers be autocatalytic in nature? Yes, this is evidenced by over a century of investigations into the nucleation phenomena of crystals, and the more recent work on supramolecular polymers, like amyloid fibrils.[1,13] There are two published mechanisms in which the supramolecular polymers in this system could generate autocatalytic kinetics/ cycles as part of their self-assembly process. These are: (i) fragmentation, which is the shearing of individual polymers into one or two "daughters" resulting in an averaged polymer length that is continuously sheared into growing smaller polymers; and (ii) detachment, where secondary nucleation on the surfaces of the polymers results in new polymers that are sheared off once a new polymer is of an appropriate size. With these facts in hand, we need now only couple the self-assembly of the supramolecular polymer to the reaction sequence, thus defining our system as autoinduction autocatalysis (Fig. 3).[1] We hypothesise that the simplest way to do this is to couple the irreversible enol–keto tautomerisation to the autocatalytic cycle (conversion of the unstable enol intermediate AB_3 to C). The alternative/related mechanism would be the surface functionality of the supramolecular polymer catalysing the formation of C via one of the four steps (causing an enhancement of secondary nucleation). This is a possibility but is rather complex in nature. A simpler mechanism can be suggested by taking into account that AB_3 and C can coassemble into supramolecular polymers as their chemical structures are significantly similar. Once formed, this new chemical environment for AB_3 (out of water) would enhance the probability of it converting to C permanently. If we then apply Le Chatelier's principle for the equilibria forming AB_3, we can ascertain that the autocatalytic cycle coupled to the coassembly would dominate the kinetics resulting in our observations, i.e., the rates of inclusion and tautomerisation are greater than the rate of disassembly of the AB_3C^P polymer.[30] Our final remark is about why B is so important to these observations and the reaction network (as similar chemistries we have reported have not been observed to show these autoinduction kinetics). The other similar aniline chemistries we have performed have not had the competitive alternative reaction pathways that we see with the alkyl amine and aniline functional groups available in B. The other aniline kinetics are far too fast to analytically determine accurately, typically taking minutes, but with the reaction competition from the alkyl amine, the reaction with B is substantially slowed to days and also provides a "convenient" set of products that do not self-assemble, thus slowing nucleation (the induction point). Future work therefore aims to take this competitive chemistry and couple it to other aniline derivatives to determine if this auto-induction can be universally applied to our reactivity of A.

Once the reaction had reached completion, the solution was acidified to induce gelation. This resulted in an increase in the concentration of the charge-neutral form of C^{n-} (C), which is likely to be part of a more complex supramolecular polymer assembly. This alters the $C^{n-}:C$ dynamic ratio with the hydrophobic, zwitterionic species C proving to be an effective low molecular weight gelator (LMWG).[31,32] C has a critical gel concentration (CGC) of 7.2 mM (0.5 wt%). Acidification of the solution was performed utilising glucono-delta-lactone (GdL) to ensure a homogenous pH change throughout the solution.[33–35] With the isoelectric point (pI) of phenylalanine (5.91) being comparable to the apparent pI of C, it is possible to understand how the addition of GdL induces gelation. At the initial pH of 9, a point which lies above the pI, C^{n-} is the dominant compound

(equilibrium) and is the more soluble form. Upon addition of GdL, the pH is slowly lowered below the pI of **C**, changing the dynamic ratio towards the more insoluble zwitterion. This insolubility gives rise to the formation of the fibrous network. The discotic nature of **C** lends itself to the one-dimensional assembly of fibres. It is a fibrous morphology that is observed by scanning electron microscopy (SEM) (Fig. S8†). It also means there is a reasonable agreement with the cellular solid model for describing the structure of supramolecular gels.[36–38] The cellular solid model predicts that $G' \propto [\text{gelator}]^n$, where G' is the elastic modulus of the gel and n can lie between 1 and 2. By performing a concentration study and examining the gels' responses to an applied oscillatory stress across a range of frequencies, the relationship $G' = 866[\textbf{C}]^{1.9}$ was obtained (see the ESI, Section 5†). This is in good agreement with the cellular solid model. This relationship allows kinetic data on the chemical reaction that produces $\textbf{C}^{n-}$ to be extracted from the mechanical properties of the produced gels. Because the reaction is performed *in situ*, a gel can be set before the final maximum concentration of **C** (or $\textbf{C}^{n-}$) is reached, provided that $[\textbf{C}] \geq$ CGC. This will result in a gel with a G' value that corresponds to the specific concentration of **C** achieved at the time of setting. This trapping out of **C** by a mass transfer limitation mechanism allows the mechanical strength of the gel in terms of G' to be predictably controlled. By changing the time at which the gel is set, under specific conditions of the reaction, we have produced gels from a single stock solution with G' values ranging from 730–2400 Pa. This results in a temporal dependence of the gels' mechanical strength with respect to the reaction rate (the rate being autocatalytic in mathematical terms). The rheological measurements can also be utilised to calculate the concentration of **C** using the cellular solid model. Doing so results in a close match in the kinetics determined through rheology to that determined by NMR and HPLC (Fig. 1).

Conclusions

In conclusion, we have developed an autoinduction reaction network that can be used predictably to produce a LMWG. This is a highly efficient template-based kinetically autocatalytic, self-replicating system that utilizes dynamic imine chemistry coupled to self-assembly. The dynamic nature of the imine bond that allows "error-checking" correction gives rise to one reaction product. This product represents a thermodynamic minimum within the system's energy landscape. The self-assembly in solution of the replicator results in the formation of supramolecular polymers, which would normally markedly reduce the catalytic efficiency of the system. This inhibiting effect can be overcome by two methods: mechanical agitation of the reaction solution and seeding the solution with a previously isolated sample of replicator. By overcoming the limiting effects of the self-assembly process, it was possible to demonstrate exponential growth in replicator concentration, thus highlighting a connection between the nucleation-based self-assembly autocatalytic cycle and the chemical reactions (imine equilibria and enol–keto tautomerisation). Not only does this study provide a basis with which to explore aspects of biochemistry and gelation connected to reaction networks, but it also explores the potential of self-replicators playing a crucial role in the origin of life being connected to their supramolecular polymer self-assembly (nucleation-based autocatalytic cycles). By controlling the kinetics of

the autocatalytic chemical reaction at one end of the hierarchical assembly process, we can influence the physical properties of the supramolecular gel at the other end. This may have wide-ranging applications with *in-situ*-formed LMWGs where a specific mechanical strength/formulation is desired.

Data availability

The data supporting this article have been included as part of the ESI.†

Author contributions

JSF and GOL provided formal analysis, data curation, investigation, methodology, project administration, validation, visualisation, and writing for this work. In addition, GOL provided supervision, resources, project administration, funding acquisition, and conceptualisation for this discussion paper.

Conflicts of interest

There are no conflicts to declare.

Acknowledgements

Notes and references

1 (*a*) W. Ostwald, Über autokatalyse, *Ber. Verh. Kgl. Sächs. Ges. Wiss. Leipzig, Math.-Phys. Classe*, 1890, **42**, 189–191; (*b*) Z. Peng, K. Paschek and J. C. Xavier, *BioEssays*, 2022, **44**, 2200098; (*c*) R. Plasson, A. Brandenburg, L. Jullien and H. Bersini, *J. Phys. Chem. A*, 2011, **115**, 8073–8085; (*d*) D. G. Blackmond, *Chem. Rev.*, 2020, **120**, 4831–4847; (*e*) D. H. Lee, K. Severin and M. R. Ghadiri, *Curr. Opin. Chem. Biol.*, 1997, **1**, 491–496; (*f*) A. I. Hanopolskyi, V. A. Smaliak, A. I. Novichkov and S. N. Semenov, *ChemSystemsChem*, 2021, **3**, e2000026; (*g*) G. A. M. King, *Chem. Soc. Rev.*, 1978, **7**, 297–316; (*h*) V. C. Allen, C. C. Robertson, S. M. Turega and D. Philp, *Org. Lett.*, 2010, **12**, 1920–1923; (*i*) K. Horváth, *Phys. Chem. Chem. Phys.*, 2021, **23**, 7178–7189.
2 J. W. Sadownik and D. Philp, *Angew. Chem., Int. Ed.*, 2008, **47**, 9965–9970.
3 B. Rubinov, N. Wagner, M. Matmor, O. Regev, N. Ashkenasy and G. Ashkenasy, *ACS Nano*, 2012, **6**, 7893–7901.
4 A. J. Bissette and S. P. Fletcher, *Angew. Chem., Int. Ed.*, 2013, **52**, 12800–12826.
5 P. Nowak, M. Colomb-Delsuc, S. Otto and J. Li, *J. Am. Chem. Soc.*, 2015, **137**, 10965–10969.

6 M. Kindermann, I. Stahl, M. Reimold, W. M. Pankau and G. von Kiedrowski, *Angew. Chem.*, 2005, **117**, 6908–6913.

7 R. F. Ludlow and S. Otto, *Chem. Soc. Rev.*, 2008, **37**, 101–108.

8 J. Li, P. Nowak and S. Otto, *J. Am. Chem. Soc.*, 2013, **135**, 9222–9239.

9 J. E. Richards and D. Philp, *Chem. Commun.*, 2016, **52**, 4995–4998.

10 S. Debnath, S. Roy and R. V Ulijn, *J. Am. Chem. Soc.*, 2013, **135**, 16789–16792.

11 J. Boekhoven, W. E. Hendriksen, G. J. M. Koper, R. Eelkema and J. H. van Esch, *Science*, 2015, **349**, 1075–1079.

12 C. G. Pappas, I. R. Sasselli and R. V Ulijn, *Angew. Chem., Int. Ed.*, 2015, **54**, 8119–8123.

13 (*a*) J. Boekhoven, A. M. Brizard, K. N. K. Kowlgi, G. J. M. Koper, R. Eelkema and J. H. van Esch, *Angew. Chem., Int. Ed.*, 2010, **49**, 4825–4828; (*b*) E. Mattia and S. Otto, *Nat. Nanotechnol.*, 2015, **10**, 111–119; (*c*) J. Boekhoven, J. M. Poolman, C. Maity, F. Li, L. van der Mee, C. B. Minkenberg, E. Mendes, J. H. van Esch and R. Eelkema, *Nat. Chem.*, 2013, **5**, 433–437; (*d*) H. A. Miers and F. Isaac, *J. Chem. Soc. Trans.*, 1906, **89**, 413–454; (*e*) J. Garside and R. J. Davey, *Chem. Eng. Commun.*, 1980, **4**, 393–424.

14 (*a*) E. Axell, J. Hu, M. Lindberg, A. J. Dear, L. Ortigosa-Pascual, E. A. Andrzejewska, G. Šneiderienė, D. Thacker, T. P. J. Knowles, E. Sparr and S. Linse, *Proc. Natl. Acad. Sci. U. S. A.*, 2024, **121**, e2322572121; (*b*) M. S. Törnquist, T. C. T. Michaels, K. Sanagavarapu, X. Yang, G. Meisl, S. I. A. Cohen, T. P. J. Knowles and S. Linse, *Chem. Commun.*, 2018, **54**, 8667–8684; (*c*) E. Axell, J. Hu, M. Lindberg and S. Linse, *Proc. Natl. Acad. Sci. U. S. A.*, 2024, **121**, e2322572121.

15 (*a*) X. Miao, A. Paikar, B. Lerner, Y. Diskin-Posner, G. Shmul and S. N. Semenov, *Angew. Chem., Int. Ed.*, 2021, **60**, 20366–20375; (*b*) C. Y. Sung, J. Estrin and G. R. Youngquist, *AIChE J.*, 1973, **19**, 957–962; (*c*) R. Schulman, B. Yurke and E. Winfree, *Proc. Natl. Acad. Sci. U. S. A.*, 2012, **109**, 6405–6410.

16 V. D. Nguyen, A. Pal, F. Snijkers, M. Colomb-Delsuc, G. Leonetti, S. Otto and J. van der Gucht, *Soft Matter*, 2016, **12**, 432–440.

17 A. Pal, M. Malakoutikhah, G. Leonetti, M. Tezcan, M. Colomb-Delsuc, V. D. Nguyen, J. van der Gucht and S. Otto, *Angew. Chem., Int. Ed.*, 2015, **54**, 7852–7856.

18 (*a*) F. Versluis, J. H. van Esch and R. Eelkema, *Adv. Mater.*, 2016, **28**, 4576–4592; (*b*) M. G. Howlett and S. P. Fletcher, *Nat. Rev. Chem*, 2023, **7**, 673–691; (*c*) J. M. Ribó, D. Hochberg, T. Buhse and J.-C. Micheau, *Phys. Chem. Chem. Phys.*, 2025, **27**, 2516–2527.

19 M. J. Webber, E. A. Appel, E. W. Meijer and R. Langer, *Nat. Mater.*, 2016, **15**, 13–26.

20 A. R. Hirst, S. Roy, M. Arora, A. K. Das, N. Hodson, P. Murray, S. Marshall, N. Javid, J. Sefcik, J. Boekhoven, J. H. van Esch, S. Santabarbara, N. T. Hunt and R. V Ulijn, *Nat. Chem.*, 2010, **2**, 1089–1094.

21 (*a*) J. S. Foster, J. M. Żurek, N. M. S. Almeida, W. E. Hendriksen, V. A. A. le Sage, V. Lakshminarayanan, A. L. Thompson, R. Banerjee, R. Eelkema, H. Mulvana, M. J. Paterson, J. H. van Esch and G. O. Lloyd, *J. Am. Chem. Soc.*, 2015, **137**, 14236–14239; (*b*) S. Ghosh, M. G. Baltussen, N. M. Ivanov, R. Haije, M. Jakštaitė, T. Zhou and W. T. S. Huck, *Chem. Rev.*, 2024, **124**(5), 2553–2582; (*c*) E. Lantos, Á. Tóth and D. Horváth, *Chaos*, 2023, **33**, 103104; (*d*) E. Lantos, G. Mótyán, E. Frank, R. Eelkema, J. van Esch, D. Horváth and

Á. Tóth, *RSC Adv.*, 2023, **13**, 20243–20247; (*e*) S. N. Semenov, L. J. Kraft, A. Ainla, M. Zhao, M. Baghbanzadeh, V. E. Campbell, K. Kang, J. M. Fox and G. M. Whitesides, *Nature*, 2016, **537**, 656–660.

22 M. E. Belowich and J. F. Stoddart, *Chem. Soc. Rev.*, 2012, **41**, 2003–2024.

23 C. V Yelamaggad, A. S. Achalkumar, D. S. Shankar Rao and S. K. Prasad, *J. Am. Chem. Soc.*, 2004, **126**, 6506–6507.

24 J. H. Chong, M. Sauer, B. O. Patrick and M. J. MacLachlan, *Org. Lett.*, 2003, **5**, 3823–3826.

25 B. G. Bag and G. von Kiedrowski, *Pure Appl. Chem.*, 1996, **68**, 2145–2152.

26 C. V. Yelamaggad, A. S. Achalkumar, D. S. S. Rao and S. K. Prasad, *J. Org. Chem.*, 2007, **72**, 8308–8318.

27 M. Colomb-Delsuc, E. Mattia, J. W. Sadownik and S. Otto, *Nat. Commun.*, 2015, **6**, 7427.

28 S. Kandambeth, A. Mallick, B. Lukose, M. V. Mane, T. Heine and R. Banerjee, *J. Am. Chem. Soc.*, 2012, **134**, 19524.

29 (*a*) G. Alagona, C. Ghio and P. I. Nagy, *Phys. Chem. Chem. Phys.*, 2010, **12**, 10173–10188; (*b*) R. Breslow, *Tetrahedron Lett.*, 1959, **1**, 22–26; (*c*) Q. P. Tran, R. Yi and A. C. Fahrenbach, *Chem. Sci.*, 2023, **14**, 9589–9599.

30 R. Edri, S. Fisher, C. Menor-Salvan, L. D. Williams and M. Frenkel-Pinter, *FEBS Lett.*, 2023, **597**, 2879–2896.

31 M. Wallace, J. A. Iggo and D. J. Adams, *Soft Matter*, 2015, **11**, 7739–7747.

32 L. Chen, K. Morris, A. Laybourn, D. Elias, M. R. Hicks, A. Rodger, L. Serpell and D. J. Adams, *Langmuir*, 2010, **26**, 5232–5242.

33 D. J. Adams, M. F. Butler, W. J. Frith, M. Kirkland, L. Mullen and P. Sanderson, *Soft Matter*, 2009, **5**, 1856.

34 E. R. Draper, L. L. E. Mears, A. M. Castilla, S. M. King, T. O. McDonald, R. Akhtar and D. J. Adams, *RSC Adv.*, 2015, **5**, 95369–95378.

35 R. C. T. Howe, A. P. Smalley, A. P. M. Guttenplan, M. W. R. Doggett, M. D. Eddleston, J. C. Tan and G. O. Lloyd, *Chem. Commun.*, 2013, **49**, 4268–4270.

36 G. O. Lloyd and J. W. Steed, *Soft Matter*, 2011, **7**, 75–84.

37 P. Terech, D. Pasquier, V. Bordas and C. Rossat, *Langmuir*, 2000, **16**, 4485–4494.

38 G. A. Buxton and N. Clarke, *Phys. Rev. Lett.*, 2007, **98**, 238103.